

1/f Magnetization Noise at the Onset of Phase Transitions for Defect Sites in SQUIDS

Amrit De¹

¹Department of Electrical Engineering, University of California - Riverside, CA 92521

(Dated: April 7, 2024)

It is shown here that $1/f^\alpha$ magnetization noise is manifestation of the onset of thermodynamic phase transitions for finite sized interfacial defects at the metal insulator interface in SQUIDS. The model comprises of clusters of interacting TLSs, likely due to color center defects. A random distribution of clusters and long range ferromagnetic interactions are shown to self consistently lead to flux noise where $\alpha(T) \lesssim 1$ over a range of temperatures in the ordered phase at the phase transition onset. The results are independent of system size and there are no prior assumptions made about the distribution of fluctuation rates. Like the experiments, the breaking of time reversal symmetry when $\alpha \sim 1$ is further confirmed through three-point correlations and flux-inductance-noise spectrum. A combination of Monte Carlo simulations and a recent method to calculate correlation functions is used in this study. The second method allows the systematic extraction of temperature dependent n^{th} -order correlation functions for N arbitrary interacting two-level-systems(TLSs). Further, from the fluctuation dissipation theorem it is shown why the experimentally observed inductance noise is inherently temperature dependent while the flux noise is not. Analytical expressions allow simplified four-point correlation function calculations.

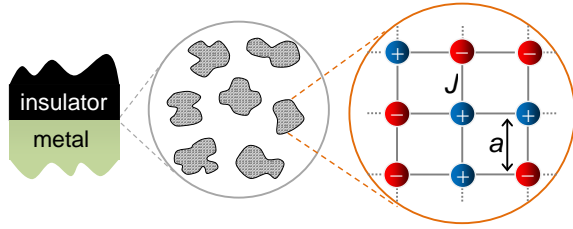


Figure 1. $1/f^\alpha$ noise model consisting of interacting and fluctuating TLSs in a cluster. The clusters are assumed to form due to random defects at the metal-insulator interface and are sufficiently far apart so that only spins within a single cluster interact. Number of TLSs within a cluster and the lattice constant a vary.

I. INTRODUCTION

Ever since its first measurement in the 1920's¹, flicker noise or $1/f$ noise has been seen in a wide variety of solid state systems²⁻⁴. Examples include spin glasses⁵⁻⁷, Coulomb glasses^{8,9}, metal films¹⁰, metal-insulator tunnel junctions¹¹⁻¹³, various semiconductor devices¹⁴ such as field-effect transistors(FETs)^{15,16}, core-shell nanowire FETs¹⁷, GaN/AlGaIn heterostructures¹⁸ and more recently in Graphene devices^{19,20}. Though there is no common physical underlying mechanism that gives rise to all these different manifestations², it has been argued by Bak that $1/f$ noise will occur in barely stable dynamical systems with extended spatial degrees of freedom²¹ which evolve into self organized critical structures.

In many solid state systems the presence of parasitic two-level-systems(TLSs), possibly due to the presence of defects, generates random-telegraphic-noise(RTN)^{22,23}. Typically if there are a large number of fluctuating TLSs then a log normal distribution of their switching rates gives rise to a $1/f$ power spectrum within some frequency range (see Appendix-B). For solid state quantum computing, $1/f$ noise is a major problem as it is a significant source of decoherence^{4,24-27}. In semiconductor quantum dots(QDs), RTN is observed when electrons

randomly tunnel back and forth²⁸⁻³⁰.

Currently superconducting quantum interference devices (SQUIDS) are at the forefront of quantum computing. SQUID based qubits are promising as they can replicate properties of natural qubits (such as electron and nuclear spins) using macroscopic devices³¹. However, the practical implementation of a scalable quantum computer based on charge-, flux-, phase- or transmon qubits is severely impeded by the presence of $1/f$ charge noise or $1/f$ magnetic noise. This limits the phase coherence of SQUID based qubits⁴.

This paper focuses on various puzzling features of $1/f$ magnetization noise in SQUIDS. In the case of flux based qubits and phase qubits, experiments have revealed that the magnetic flux noise has a $1/f$ -type power spectrum^{32,33}. Although, this type of magnetic flux noise was first observed in SQUIDS in the 80's^{34,35}, its origins were not fully explained. The interest in this subject has however been revived because of the recent activity in quantum computing. A better understanding of the microscopic origins of this noise could lead to better Josephson tunnel junction designs³⁶ and possible elimination of a source of contamination in SQUIDS. It has been shown the magnetic noise can be reduced by appropriate surface treatment³⁷.

Magnetic noise in SQUIDS have several key features. Amongst them is that the flux noise is only weakly dependent on geometry. Recent measurements on qubits with different geometries indicate that the flux noise scales as l/w , in the limit $w/l \ll 1$ (where l is the length and w is the width of the superconducting wires)³⁸. This along with recent experiments by Sendelbach *et al*³⁹ suggests that flux noise arises from unpaired surface spins which reside at the superconductor-insulator interface in thin-film SQUIDS. The estimated areal spin density from the paramagnetic susceptibilities, for superconductor-insulator³⁹ interfaces (and metal-insulator⁴⁰ interfaces) is about $5 \times 10^{17} \text{ m}^{-2}$. As a result of this high spin density, the coherent magnetization of the spins results in a large flux coupling to the SQUID.

Another key feature of this flux noise is that it is only weakly dependent on parameters such as temperature,

choice of the superconducting material and the area of the SQUID^{34,41}. In addition to the flux noise, the inductance noise was also measured in the experiments of Ref.39. It was seen that inductance noise, which scales as $1/f^\alpha$, decreases with increasing temperature and α itself is temperature dependent ($0 < \alpha(T) < 1$)⁴².

This deduced areal density is consistent with some of the theoretical models such as in terms of metal induced gap states that arise due to the potential disorder at the metal-insulator interface⁴³. Several models have been suggested including non-interacting electron hopping between traps with different spin orientations and a $1/f$ distribution of trap energies⁴⁴, a dangling bond model⁴⁵ and interacting fractal spin clusters with varying number of spins to obtain a $1/f$ distribution of relaxation rates⁴⁶ and a flux-vector model⁴⁷. Sometime ago Kozub⁴⁸ proposed a model where the amplitude of $1/f$ noise scaled as $1/T$, however this model did not consider spin-spin interactions.

Experimental evidence on the other hand suggests that these surface spins are strongly interacting and that there is a net spin polarization³⁹. It is seen that the $1/f$ inductance noise is highly correlated with the usual $1/f$ flux noise. Their cross-correlation is inversely proportional to the temperature and is about the order of unity roughly below $T \approx 100\text{mK}$. Now inductance is even under time inversion whereas flux is odd under time inversion. This implies that their three-point cross-correlation function must be zero unless time inversion symmetry is broken. This is only possible only by the appearance of long range magnetic ordering, unless an external magnetic field is applied. The mechanism producing both the flux noise and inductance noise is expected to be the same.

It has been suggested that the spins at the superconductor-insulator interface interact with each other via the RudermanKittelKasuyaYosida (RKKY) mechanism⁴⁹ which is responsible for the spin polarization reported in experiments³⁹. The RKKY interaction can give rise to unusual magnetic ordering in SQUIDs as the magnetic ordering can oscillate between being ferromagnetic to being antiferromagnetic as a function of distance. Antiferromagnetic RKKY interactions can give rise to a spin glass type phase and $1/f$ noise related to the magnetic fluctuations and low temperature kinetics^{5-7,50-52}.

However Monte-Carlo simulations⁵³ have ruled out the formation of a spin glass phase to explain magnetization noise in SQUIDs. It was shown that an Ising-type spin glass with random nearest neighbor interactions can reproduce qualitative features of the temperature dependent inductance noise, but does not show cross-correlations between inductance and flux noise. This is expected in spin glasses where the time reversal symmetry is preserved due to zero net magnetic moment. This leads to a vanishing three-point cross-correlation function between magnetization and susceptibility.

In a related development, a few years ago surface ferromagnetism (SFM) was reported in thin-films and nanoparticles of a number of otherwise insulating metallic oxides⁵⁴ (including Al_2O_3) where the materials were not doped with any magnetic impurities. Further recent investigations attribute this room temperature SFM in Al_2O_3 nanoparticles⁵⁵ to F^+ -

center where it was found that amorphous Al_2O_3 is more likely to host the number of F^+ -centers to cross the magnetic percolation threshold than the crystalline variant. The origin of SFM in these otherwise non-magnetic metal oxides is itself somewhat controversial⁵⁶ where a number of different exchange coupling mechanisms have been proposed⁵⁷⁻⁵⁹.

SFM and the SQUID geometry provides some important clues on the microscopic origins of the $1/f$ flux noise. Typically dc-SQUIDs have an amorphous Al_2O_3 insulating layer deposited on the surface of a metal (commonly Nb³⁹ or Al³³). Al_2O_3 is likely to cluster on the surface before filling in and forming a homogeneous layer due to its higher binding energy which could lead to the Volmer-Weber growth mode. The lattice mismatch between the insulator and the metal could also lead to the formation of clusters. Near the metal surface, the clusters can host a number of point defects in the form of O vacancies that can capture one electron – F^+ -center, or two (F-center). Surface absorption of O_2 ^{37,60}, intrinsic vacancies⁶¹ and even hydrogen⁶² are among some of the suggested origins of the magnetic moments responsible for the flux noise. In addition to this, in the SQUID geometry because of the proximity to the metal, these local magnetic moments can spin polarize the metal's conduction band electrons which can lead to an RKKY type long range interaction⁴⁹. This can lead to competing interaction mechanisms.

A temperature dependent spin-cluster model with ferromagnetic interactions was proposed recently to explain various puzzling features of $1/f$ magnetization noise in SQUIDs⁶³. This spin-cluster model explains various experimental results self consistently and is representative of a disordered system at the SQUID's metal-insulator interface (see fig.1). Additional model calculations and newer results are presented in this paper.

An important connection is made here between the noise exponent α and phase transitions. It is found here that the $\alpha(T)$ is less than 1 and relatively independent of temperature over a short range in the ordered phase as the system heads into a thermodynamic phase transition. α drops rapidly as the system enters the disordered phase. Further clues are provided while trying to explain the measured flux-inductance noise cross correlations. Time reversal symmetry is shown to be spontaneously broken at low temperatures from three-point flux noise and inductance noise cross-correlation calculations. All of this is done using a careful combination of Monte-Carlo simulations with parallel tempering and a newer correlation function calculation method.

A method is suggested to systematically extract any n^{th} order correlation function for N interacting Ising spins, within the framework of Ising-Glauber dynamics. Detailed discussions are presented in this paper. Analytical results are provided for easier calculation of 2-point and 4-point correlations functions and power spectra. Overall this method is well suited for numerics as well as for analytics in smaller systems, and is inspired by the quasi-Hamiltonian open quantum systems formalism^{27,64-69}.

In the case of the interaction dependent model presented here, as such no *a priori* heuristic assumptions are made for a log-normal distribution of fluctuation rates that lead

to $1/f$ noise. Instead, $1/f^\alpha$ noise (with $\alpha < 1$ like the experiments³⁹) is shown to manifest naturally from the combination of long range ferromagnetic interactions and multiple clusters with a normal random distribution of lattice constants. Furthermore this noise is shown to be independent of system size – similar to experiments. And it is shown that ferromagnetic short-range-mechanisms will lead to flux noise that varies considerably more with temperature when compared to clusters with long range interactions.

The second spectrum (or the noise of the noise) is also extensively discussed here. This is the inductance noise. It is not so obvious why, the experimentally measured second spectra shows a huge temperature dependence while the first spectrum doesn't even though they have the same underlying noise microscopics. Here it is analytically shown why the measured inductance noise inherently has a huge T^{-2} temperature dependence even though the flux noise (first spectrum) may not.

This paper is organized as follows. In section-2 the model and the correlation function calculation technique is discussed. In section-3, the Monte-Carlo phase transitions results are compared against the noise exponent. This is followed by flux-inductance noise cross-spectral results (three point correlations) in section-4. The inductance noise calculations along with various analytical expressions are presented in section-5 followed by the summary. Appendix-A gives an explicit analytical expressions for a pair of interacting TLSs.

II. METHOD: CORRELATION FUNCTIONS FROM ISING-GLAUBER DYNAMICS

Fluctuating two level systems can be treated as Ising spins which flip randomly in time. Their stochastic dynamics is therefore governed by the master equation⁷⁰,

$$\frac{d\mathbf{W}(t)}{dt} = \mathbf{V}\mathbf{W}(t) \quad (1)$$

where \mathbf{V} is a matrix of transition rates (such that the sum of each of its columns is zero) and \mathbf{W} is the flipping probability matrix for the TLS. For N TLS, \mathbf{V} and \mathbf{W} are $2^N \times 2^N$ matrices.

For correlated spin fluctuations, the system's overall temporal dynamics is also governed by the master equation Eq.1. The Ising-Glauber model (also known as the kinetic Ising model) can be used to treat the non-equilibrium dynamics for fluctuating spins^{71,72}. Single-site Glauber dynamics requires that a single spin is flipped at a given site, and that the new configuration agrees with the old one everywhere except where the spin was flipped. This is a Markov process where the new distribution of spins depends only on the current spin configuration. And for Glauber dynamics, the conditional probability for a spin to flip is determined by the Boltzmann factor. The matrix-elements of \mathbf{V} for correlated spin

flips are therefore

$$\mathbf{V}(\mathbf{s} \rightarrow \mathbf{s}') = \begin{cases} \frac{\gamma e^{-\beta H(\mathbf{s}')}}{e^{-\beta H(\mathbf{s})} + e^{-\beta H(\mathbf{s}')}} & \text{for } \mathbf{s} \neq \mathbf{s}' \text{ and} \\ & \sum_i (1 - s_i s'_i) = 2 \\ - \sum_{\mathbf{s} \neq \mathbf{s}'} \mathbf{V}(\mathbf{s} \rightarrow \mathbf{s}') & \text{for } \mathbf{s} = \mathbf{s}' \end{cases} \quad (2)$$

Here, \mathbf{s}' is a vector denoting the present spin configuration of the lattice, \mathbf{s} denotes the spin configuration of the lattice at an earlier instance of time and γ is the relaxation rate of the spin that is flipped. The non negative off-diagonal matrix elements in Eq.2 satisfy the detailed balance condition and the diagonal terms is the just negative sum of the off-diagonal column elements so that all column elements sum up to zero, which ensures the conservation of probability. The systems temporal dynamics is then governed by the flipping probability matrix, which is $\mathbf{W} = \exp(-\mathbf{V}dt)$. The eigenvalues of \mathbf{V} are either zero, which corresponds to the equilibrium distribution, or are real-negative which also eventually tend to the equilibrium distribution as time $t \rightarrow \infty$ ⁷⁰.

The overall system Hamiltonian in the Boltzmann factor in Eq.2 is

$$H(\mathbf{s}) = -\frac{1}{2} \sum_{i,j} J_{i,j} s_i s_j - B \sum_i s_i \quad (3)$$

where B is the magnetic field and $J_{i,j}$ is the spin-spin interaction between the i^{th} and j^{th} spins.

Now for N spins (either interacting or non-interacting), any n^{th} order correlation function between arbitrary spins can be *exactly* calculated as follows

$$\langle s_\ell(t_1) s_j(t_2) \dots s_\kappa(t_n) \rangle = \langle f | \sigma_z^{(\kappa)} \mathbf{W}(t_n) \dots \sigma_z^{(j)} \mathbf{W}(t_2) \sigma_z^{(\ell)} \mathbf{W}(t_1) | i \rangle \quad (4)$$

where it is implied that

$$\sigma_z^{(\kappa)} = \sigma_{o_1} \otimes \sigma_{o_2} \dots \sigma_{o_{\kappa-1}} \otimes \sigma_z \otimes \sigma_{o_{\kappa+1}} \dots \otimes \sigma_{o_N} \quad (5)$$

And it is assumed that \mathbf{W} and $\sigma_z^{(\kappa)}$ are in the same lexicographically ordered Ising spin basis.

III. RESULTS AND DISCUSSION

A. First Spectrum: Flux Noise

Because of the high estimated areal spin density, the coherent magnetization of the spins strongly flux couples to the SQUID. The fluctuation-dissipation theorem relates the magnetization noise spectrum to the imaginary part of the susceptibility $P(\omega) = 4\chi''(\omega)/\beta\omega$ ^{41,73,74}. If all the surface spins couple to the SQUID equally, the flux noise from the ℓ^{th} spin-cluster is

$$P_\phi^{(\ell)}(\omega) = 2\mu_o^2 \mu_B^2 \frac{\rho}{\pi} \frac{R}{r} \int_0^\infty \sum_{i,j=1}^N \langle s_i(0) s_j(t) \rangle e^{i\omega t} dt \quad (6)$$

where R is the radius of the loop, r is the radius of the wire, $R/r = 10^{41}$ and ρ is the surface spin density.

Using Eq.5, $\sum \langle s_i(0)s_j(t) \rangle = \langle \mathbf{f} | \sigma^i \mathbf{W}(t) \sigma^j \mathbf{W}(0) | i \rangle$ is calculated by considering all possible combinations of two-point autocorrelation functions ($i = j$) and cross-correlation ($i \neq j$) functions for a given cluster. Here \mathbf{W} is a $2^{N_j} \times 2^{N_j}$ flipping probability matrix. Each cluster is assumed to be sufficiently far apart and noninteracting and the total flux noise power is

$$P_\phi(\omega) = \sum_{\ell} P_\phi^{(\ell)}(\omega) \quad (7)$$

At finite temperatures, for two interacting spins in the $\gamma_j = 1$ limit, it can be analytically shown (see Appendix) that the correlation functions are:

$$\langle s_i(0)s_j(t) \rangle = \frac{1}{2}e^{-2\Gamma'_-|t|} + \left(\delta_{ij} - \frac{1}{2} \right) e^{4\beta J} e^{-2\Gamma'_+|t|} \quad (8)$$

where $\Gamma'_\pm = [1 + \exp(\pm 2\beta J)]^{-1}$. Note that $\sum_{i,j} \langle s_i(0)s_j(t) \rangle = 2e^{-2\Gamma'_-|t|}$. In this case the two interacting TLS behave like a single quasi-spin with effective flipping rate Γ'_- . It can be argued that the sum of all two-point correlation functions for an arbitrary number of interacting spins can always be expressed as

$$\sum_{i,j} \langle s_i(0)s_j(t) \rangle = \sum_{\nu} C_\nu e^{-2\Gamma_\nu t}. \quad (9)$$

This is verified numerically in fig.2 where the fits are shown to be in exceptionally good agreement with the calculations.

For numerics, fitting the net correlation functions to Eq.9 first has a number of advantages too. In the case of ferromagnetic interactions, the correlations functions can be very long lived at low temperatures. This can be a significant problem when one is trying to numerically obtain the Fourier transform for the noise power spectrum. Instead if the fitted form in Eq.9 is used, then the Fourier transform can be obtained semi-analytically, where the power spectrum will just be a sum of Lorentzians weighted by C_ν .

The temperature dependent net correlation function, power-spectrum of the flux noise, $P_\phi(\omega)$, and its respective slope is shown in Figs.3(a)-(c). For these calculations 75 spin clusters were considered where each cluster has a random $k_F a$ and between 6-9 spins. The normalized lattice constants ($k_F a$) were uniformly distributed as shown in Fig.3-(d). If Eq.??, expanded upto second order for small $k_F a$, then one can see that:

$$J_{i,j} \propto \frac{1}{k_F R_{ij}} \quad (10)$$

Hence this implies that a uniform distribution of the lattice constants results in roughly a $1/J_{i,j}$ distribution of interaction strengths.

From the experimentally estimated areal surface spin density of $\rho \sim 5 \times 10^{17} m^{-2}$ ^{39,40}, one can estimate k_F and the average spin separation $\langle a \rangle$. Note that these results are independent of the cluster size or the number of spins in a cluster. In

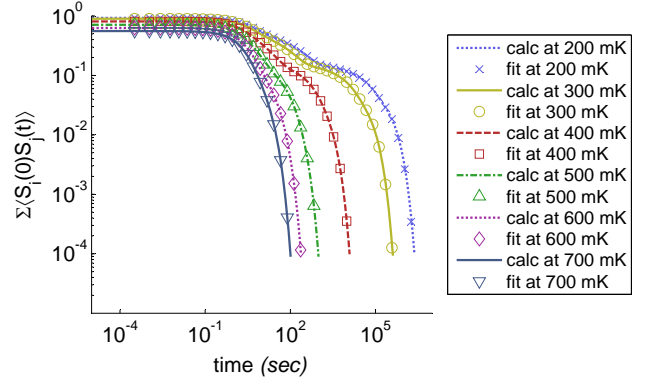


Figure 2. (a) Comparison between calculated net correlation functions and fits to $\sum C_\nu \exp(-\Gamma_\nu t)$ at various temperatures. The fits are in perfect agreement with the calculations done for 50 spin clusters, each with 7 spins.

Fig.4, the noise spectra calculations are repeated for 20 clusters, with 6 spins per cluster. It can be seen that the noise spectra in Fig.4 is qualitatively very similar to that of Fig.3. This is consistent with experiments where the flux noise was seen to be more or less independent of the area of the SQUID^{34,41} or the cluster size.

As shown in Figs.3 (c) and 4 (c), at very high frequencies, the $1/f^\alpha$ flux noise power spectra has a slope of 2 which corresponds to the Lorentzian tail of the noise power. For an intermediate range of frequencies, a region of slope ($\alpha < \sim 1$) is seen at the highest temperature. Eventually for all temperatures, $\alpha \rightarrow 0$ at very low frequencies which corresponds to gaussian noise.

Here the $1/f^\alpha$ noise (with $\alpha < 1$ like the experiments³⁹) is shown to manifest naturally from the combination of long range ferromagnetic interactions and multiple clusters with a normal distribution of lattice constants. In the infinite temperature limit or if the interactions are turned off for these calculations, then the same distribution of $k_F a$ results in just a simple Lorentzian power spectra. Finally, the upper and lower frequency cutoffs for the $1/f$ type behavior depends on the distribution of $k_F a$ and the interaction strength – which is also evident from the temperature dependence in Figs.3 and 4.

To get a better understanding of the role of the interactions and the cluster-size randomness, we next consider a nearest-neighbor interaction (NNI) model with ferromagnetic interactions for each cluster. The ferromagnetic interaction strength was of the order of J_o and depends on the distance between nearest neighbors and hence varies randomly. The NNI model also results in a $1/f$ noise spectrum as shown in Fig.5. This is similar to the case of the RKKY interactions which although oscillate between being ferromagnetic to being anti-ferromagnetic - the neighboring spins will always experience a large ferromagnetic interaction (if $J_o < 1$ and for small $k_F a$). However, the variations with temperature are larger for the case of the NNI model as finite size effects are more pronounced for the small spin clusters considered here. For the NNI, $1/f$ noise type behavior is obtained here only for one

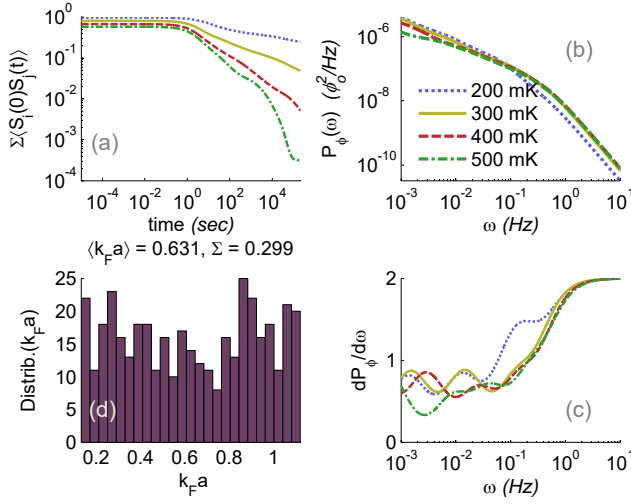


Figure 3. **(a)** Net correlation function for 400 spin clusters, each with 6-9 spins. **(b)** The corresponding power-spectrum for the flux noise, P_ϕ and **(c)** the slope of the flux noise. **(d)** Shows the distribution of $k_F a$ for each spin cluster. The mean and standard deviation (Σ) are as indicated.

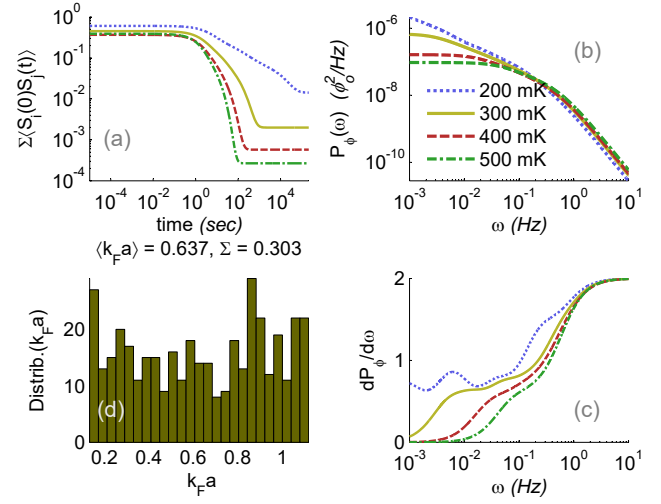


Figure 5. Calculations for spin-clusters with nearest neighbor ferromagnetic interactions showing the **(a)** net correlation function. **(b)** the corresponding power-spectrum for the flux noise and **(c)** the slope of the flux noise. **(d)** Shows the distribution of $k_F a$ for each spin cluster. The mean and standard deviation (Σ) are as indicated. The calculations are for 400 clusters with 6-9 spins.

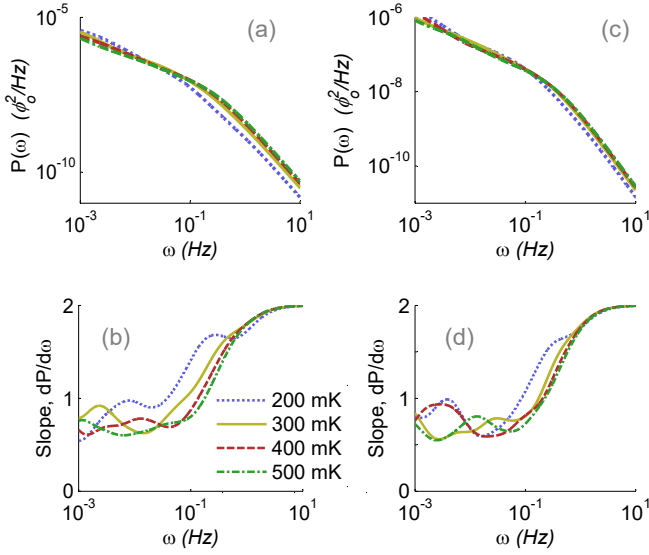


Figure 4. Power spectrum comparison for different cluster sizes. **(a)** Power spectrum and **(b)** corresponding noise slope for 75 cluster with 6-9 spins. **(c)** Power spectrum and **(d)** corresponding noise slope for 20 clusters with 6 spins.

temperature value, whereas experimentally this behavior was observed over a wide range of temperatures with almost no variation^{34,39,41}. Hence the ferromagnetic NNI model can be ruled out.

B. Monte Carlo Simulations: Fluctuations Near Phase Transition and $1/f^\alpha$ Noise

Here we examine how the flux noise's slope, α , changes with temperature and how it compares to the thermodynamic phase transitions for the interacting spin clusters. For the phase transition calculations, the temperature dependent order parameters were obtained from Monte Carlo simulations with the inclusion of parallel-tempering. The order parameters were specific heat $C_v = (\langle E \rangle^2 - \langle E^2 \rangle)/T^2$ and susceptibility $\chi = (\langle M \rangle^2 - \langle M^2 \rangle)/T$, where E is the total energy and M is the magnetization.

For the Monte-Carlo simulations, first a complete sweep of all the TLS in all lattices was taken at various temperatures. Here unlike NNI models, since RKKY interactions are involved, while updating a spin configuration, the acceptance decision is made based on the energy of the entire interacting cluster. This is numerically feasible for all systems sizes considered here. Next for the parallel tempering part, the different replicas at different temperatures was swapped using the detailed balance condition: $\min(\mathcal{R}, \exp[(E_1 - E_2)(T_1^{-1} - T_2^{-1})/k_B])$, where $0 < \mathcal{R} < 1$ is random. The whole process was repeated over 10^4 times.

The noise slope is obtained from the flux noise spectra using the correlation-function calculation method described in the earlier section

$$\alpha(T, \omega) = \frac{dP_\phi}{d\omega}, \quad (11)$$

The frequency dependence can be integrated out within a fi-

nite spectral window where $\alpha \sim 1$ at low temperatures,

$$\alpha(T) = \frac{1}{\omega_u - \omega_l} \int_{\omega_l}^{\omega_u} \alpha(T, \omega) d\omega. \quad (12)$$

Since the following comparisons between phase transitions and α involved two different calculation methods, a number of steps were taken for the calculations to be fully consistent. Exactly the same spin-cluster configuration and seeds for random-number-generation was used to generate the $k_F a$ distribution for both methods. Both Monte-Carlo and $\alpha(T)$ calculations were done for 75 spin clusters, each with 6-9 spins and a uniform distribution was chosen for $k_F a$.

The order parameters C_v and χ are shown in fig.6 along with α as a function of temperature. A close up view of α over a narrower range of temperatures is shown in the figure insets. A second order phase transition is clearly seen in fig.6-(a) and (b) where the phase transition takes place at $T \approx 1.2 J k_B^{-1} = T_c$.

As shown in the figure, there is a certain range of temperatures over which α does not vary much. $\alpha \sim 0.8$ upto the onset of the phase transition when the system is more in the ordered phase. This range of temperatures over which α remains relatively constant depends on the range of frequencies over which $\alpha(T, \omega)$ is integrated. This magnetic ordering of the system will be further verified later using three-point correlation function calculations. As the system heads towards the critical temperature (T_c), the magnetization of the clusters begin to dissipate and α rapidly drops towards 0.

This behavior is not too surprising since it was shown earlier that the interactions are necessary for $1/f^\alpha$ noise, which gives the spin cluster model its magnetic order. The noise is due to the fluctuations that occur at the onset of the thermodynamic phase transition process. Higher temperatures will wash out the interactions and hence α falls rapidly. As the system heads towards a spin glass phase at the lowest temperature α tends to rise towards 1. Note that at very low temperatures it is very difficult to extract α as the correlations times are extremely long.

Note that in this particular case for clusters with 6 – 9 spins the phase transition takes place at $T \approx 1.2 J k_B^{-1}$. This is because we are only considering small clusters of spins and T_c will be lower because of finite size effects. Fig.7 shows the critical temperature as a function of system size, N (or a single cluster) for various normalized lattice constants $k_F a$. These were obtained from Monte Carlo simulations. Because of the RKKY interactions, T_c is very sensitive to $k_F a$ and N for small sized systems. Whereas in 2D NNI Ising models, $T_c \sim 2.2 J k_B^{-1}$.

Overall this comparison indicates that $1/f^\alpha$ noise is due to the spin (or TLS) fluctuations during the onset of the phase transition process. This $1/f^\alpha$ noise occurs when the spins are fluctuating but the system is still in the ordered phase close but headed towards criticality. This is somewhat reminiscent of Bak's²¹ argument that $1/f$ noise will occur in barely stable dynamical systems with extended spatial degrees of freedom which evolve into self organized critical structures.

Overall this model explains the temperature dependence of α seen in flux noise experiments^{34,39,41} for different tem-

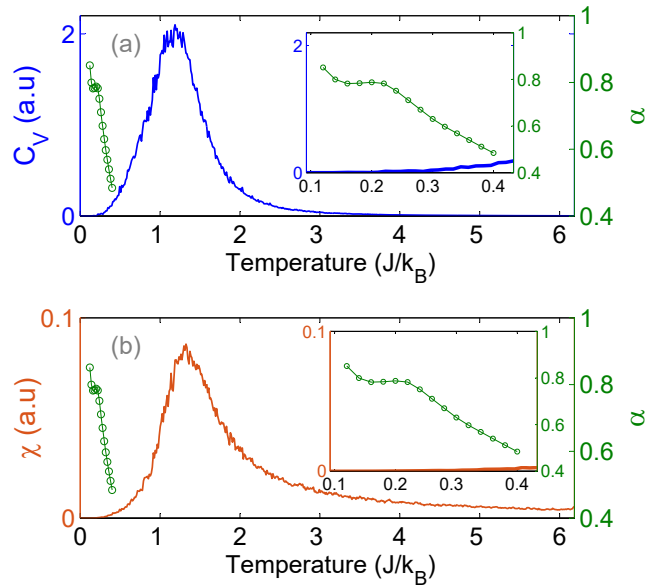


Figure 6. Comparison of the noise slope, α , against the (a) specific heat, C_v and (b) magnetic susceptibility, χ for 75 spin clusters, each with 6-9 spins. C_v and χ are calculated using the Monte-Carlo method. The same random-number seed and spin-configurations were used for calculating α . In the insets, a segment of the temperature axis is magnified to show a close-up of α .

perature and material regimes. In the experiments it was observed that the flux noise was almost independent of temperature^{34,39,41}. However it should be mentioned in some of the early experiments in the 80's³⁵ it was found that the flux noise was not necessarily independent of temperature under *all* circumstances. While there was no temperature dependence for the flux noise below 1K, there is a low temperature dependence for certain parameters and materials, such as for PbIn/Nb and Pb/Nb³⁵. Quite strikingly, for the same set of used materials (i.e. PbIn/Nb for the SQUID's loop/electrode), the flux noise can be either independent of temperature or inversely proportional to it or even oscillatory as a function of temperature depending on the construction. Such conflicting temperature dependence of $1/f$ noise is not uncommon for glassy systems. For example the $1/f$ noise amplitudes in REF.5 and REF.75 has completely opposite temperature dependencies.

Here we argue that much of this oscillatory $\alpha(T)$ behavior arises when the frequency dependence is retained in α . In figs 3 (c) and ?? (c) it can be seen that for any particular frequency slice, α is not completely constant and shows some sort of oscillatory type behavior as a function of temperature, which is similar to Ref:-35. This variation though is small. This sort of behavior is expected for the spin cluster model with ferromagnetic RKKY interactions considered here, if the lattice constant is small, *i.e* the spins are very close to each other then the effects of the RKKY interaction are more apparent. At short length scales the temperature more drastically affects α and its temperature dependence can be oscillatory. How-

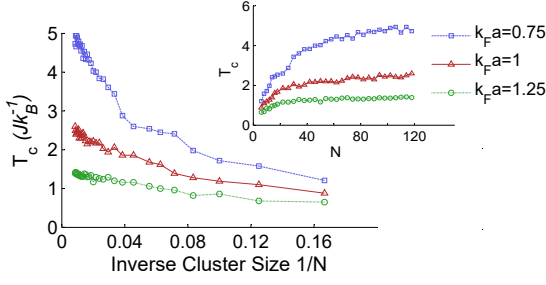


Figure 7. Critical temperature, T_c , for the spin clusters with RKKY interactions as a function of inverse cluster size, $1/N$ for various normalized lattice spacing $k_F a$. Inset shows T_c as a function of N .

$$P_{L\phi}(\omega) = \frac{1}{k_B T} \left(2\rho\mu_0^2\mu_B^2 \frac{R}{r} \right) \int_{\omega_a}^{\omega_b} \int_0^{\infty} \sum_{i,j,k} \langle s_i(t_1)s_j(t_2)s_k(t_3) \rangle e^{i\omega-\tau} e^{i\omega+\tau'} d\tau d\tau' d\omega' \quad (13)$$

where, $\tau = t_2 - t_1$, $\tau' = t_3 - t_2$, $\omega_{\pm} = \omega \pm \omega'$ and $\omega_b - \omega_a$ defines the bandwidth. In the experiments $P_{L\phi}$ was found to be inversely proportional to T and ~ 1 roughly below $100mK$ and $P_{L\phi}$ depends on the sum of all three-point correlation functions (3pt-CF). As inductance is even under time inversion and magnetic flux is odd, the flux-inductance-3pt-CF can only be nonzero if time reversal symmetry is broken – indicating the appearance of long range magnetic order. This indicates that the interactions must be ferromagnetic.

To show this, the 3pt-CF (for all possible spin combinations) is calculated by for a single cluster of 9 spins with ferromagnetic RKKY interactions, which gives $\sum \langle s_i s_j s_k \rangle_{max} \sim 1$ at low T and keeps decreasing with increasing T (see Fig.8). This is in excellent agreement with experiment and strongly indicates that the same mechanism produces both the flux noise and inductance noise. Whereas if J_o is antiferromagnetic then $\sum \langle s_i s_j s_k \rangle_{max} \sim 0$. The power spectrum for these 3pt-CFs is normalized for easier comparison and is shown in fig.8-(d). From the 3pt-CFs it can be seen that the raw power spectrum would vary considerably. The power spectrum here for a just single cluster is relatively flat.

D. Second Spectrum: Inductance Noise

This section discusses various features of the inductance noise, P_L which is the associated noise spectrum or the second spectrum. It is a quantitative measure of the spectral wandering of the first spectrum and is interpreted as the noise of the noise⁷⁶. In the experiments of Ref.39, P_L was measured below $2K$ and varied considerably with temperature. Despite having the same noise microscopics, it is not obvious why the

ever when the frequency dependence is integrated out, the α does not vary much over a wide range of temperatures upto criticality as shown in fig.6.

C. Flux-Inductance Noise Cross Spectrum and Three Point Correlations

In the earlier section it was shown that $\alpha \sim 0.8$ upto criticality when the system is more in the ordered phase. In this section we conclusively show that the TLS are magnetically ordered using three point correlation function calculations. The SQUID's surface spins show a net polarization in the experiments³⁹ as the $1/f$ inductance noise was found to be highly correlated with the $1/f$ flux noise.

The following expression gives the flux- and inductance noise cross power spectrum

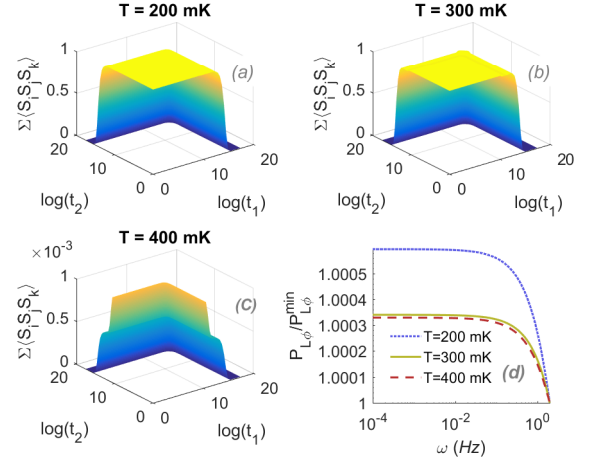


Figure 8. Sum of all three-point auto-correlation and cross-correlation functions, $\sum_{i,j,k} \langle s_i(0)s_j(t_1)s_k(t_2) \rangle$, for $N = 9$ spins with ferromagnetic RKKY interactions at (a) $T = 200 mK$ (b) $T = 300 mK$ and (c) $T = 400 mK$ where note that the z-axis is 10^3 times smaller. (d) shows the corresponding normalized power spectrum.

second spectrum should have this strong temperature dependence while the flux noise (first spectrum) does not vary with temperature. It is analytically shown here why this is the case.

The flux noise is related to the imaginary part of the susceptibility via the fluctuation-dissipation theorem

$$P(\omega) = 2\hbar \coth \left(\frac{\hbar\omega}{k_B T} \right) \chi'' = \lim_{k_B T \gg \hbar\omega} 2 \frac{k_B T}{\omega} \chi'' \quad (14)$$

Assuming all spins couple to the SQUID equally^{27,41}, the imaginary part of the inductance then relates to the spin susceptibility within a layer of thickness d on the surface as follows

$$L'' = \mu_o d \frac{R}{r} \chi'' \quad (15)$$

where L'' is the imaginary part of the inductance. If ρ is the surface spin density then $d = \rho/\tilde{n}$, where \tilde{n} is the spin density. Therefore again from the fluctuation dissipation theorem,

$$\chi''(\omega) = 2 \frac{\tilde{n} \mu_o \mu_B^2 \omega}{k_B T} \sum_{i,j} \int_0^\infty \langle s_i(0) s_j(t) \rangle e^{i\omega t} dt. \quad (16)$$

It is argued here that the sum of all two-point correlation functions for the system of interacting spins can always be expressed as

$$\sum_{i,j} \langle s_i(0) s_j(t) \rangle = \sum_{\nu} C_{\nu} e^{-2\Gamma_{\nu} t}. \quad (17)$$

This is shown analytically for two spins (see Eq.48) and systematically verified for more numerically. Hence

$$\chi''(\omega) = 2 \tilde{n} \mu_o \mu_B^2 \frac{\omega}{k_B T} \sum_{\nu} \frac{C_{\nu} \Gamma_{\nu}}{\Gamma_{\nu}^2 + \omega^2} \quad (18)$$

$$S^{[2]}(\omega, \omega_1, \omega_2) = \iiint_0^\infty \sum_{j,k,l,m} \langle s_j(t_1) s_k(t_2) s_l(t_3) s_m(t_4) \rangle e^{i(\omega_a - \omega)\tau'} e^{i(\omega_b + \omega)\tau''} e^{i\omega\tau} d\tau' d\tau'' d\tau \quad (24)$$

here $\tau' = t_2 - t_1$, $\tau'' = t_4 - t_3$ and $\tau = t_4 + t_3 - t_2 - t_1$, $\Delta\omega = \omega_b - \omega_a$ is the bandwidth within which the second spectrum is observed and j, k, l, m are spin indices.

Numerical second spectrum calculations can be considerably difficult. The four-point correlations functions have to be approximated in order to make these calculations feasible. In general for non-Gaussian noise, for any four set of arbitrary spins on a lattice: $\langle s_j(t_1) s_k(t_2) s_l(t_3) s_m(t_4) \rangle \neq \langle s_j(t_1) s_k(t_2) \rangle \langle s_l(t_3) s_m(t_4) \rangle$. In fact their differences can be quite significant. However it can be numerically shown that if the sum over all possible combinations of spins on a lattice is

$$P_L^{[2]}(\omega) = \delta(\tau) \left(2\rho \frac{\mu_o \mu_B^2 R}{k_B T r} \right)^2 \left| \left(\sum_{\nu} C_{\nu} \log \left[\frac{\omega_b + \omega + 2i\Gamma_{\nu}}{\omega_a + \omega + 2i\Gamma_{\nu}} \right] \right) \left(\sum_{\nu} C_{\nu} \log \left[\frac{\omega_b - \omega + 2i\Gamma_{\nu}}{\omega_a - \omega + 2i\Gamma_{\nu}} \right] \right) \right| \quad (27)$$

$P_L^{[2]}$ looks similar to a Lorentzian spectral function where its

and the real part from Kramers-Kronig relation is

$$\chi'(\omega) = \frac{2}{\pi} \mathcal{P} \int_0^\infty \frac{\chi''(\omega')}{\omega'^2 - \omega^2} d\omega' \quad (19)$$

$$= \frac{2\tilde{n}\mu_o\mu_B^2}{k_B T} \sum_{\nu} \frac{C_{\nu}\Gamma_{\nu}^2}{\Gamma_{\nu}^2 + \omega^2}. \quad (20)$$

where, \mathcal{P} is Cauchy's principal value. Hence from the total susceptibility $\chi(\omega) = \chi'(\omega) + i\chi''(\omega)$:

$$\chi(t) = \int_0^\infty \chi(\omega) e^{i\omega t} d\omega = \frac{2\tilde{n}\mu_o\mu_B^2}{k_B T} \sum_{i,j} \langle s_i(0) s_j(t) \rangle. \quad (21)$$

The real part χ' has to be considered in order to show this T^{-1} dependence analytically.

The inductance noise can be generally expressed as

$$P_L(\omega) = \left(\mu_o d \frac{R}{r} \right)^2 \int_0^\infty \langle \chi(0) \chi(t) \rangle e^{i\omega t} dt \quad (22)$$

The inductance noise can then be further explicitly expressed in terms of the spectral density of the dynamical four-point noise correlation functions²²,

$$P_L^{[2]}(\omega) = \left(2\rho \frac{\mu_o \mu_B^2 R}{k_B T r} \right)^2 \iint_{\omega_a}^{\omega_b} S^{[2]}(\omega, \omega_1, \omega_2) d\omega_1 d\omega_2 \quad (23)$$

where

taken, then to an excellent approximation

$$\sum_{j,k,l,m} \langle s_j(t_1) s_k(t_2) s_l(t_3) s_m(t_4) \rangle \quad (25)$$

$$\approx \sum_{j,k,l,m} \langle s_j(t_1) s_k(t_2) \rangle \langle s_l(t_3) s_m(t_4) \rangle.$$

The right hand side of Eq.26 can be split into the sum of all two-point correlation functions, which have the form of Eq.48. Therefore

$$S^{[2]}(\omega, \omega_1, \omega_2) = \delta(\tau) P'(\omega, \omega_a) P'(\omega, \omega_b) \quad (26)$$

where $P'(\omega, \omega_{a(b)}) = \sum_{\nu} C_{\nu} [2\Gamma_{\nu} + i(\omega - \omega_{a(b)})]^{-1}$. Substituting this into Eq.23, the following expression is obtained for the associated spectrum of correlated Ising spin fluctuations.

amplitude is determined by $\Delta\nu = \omega_b - \omega_a$.

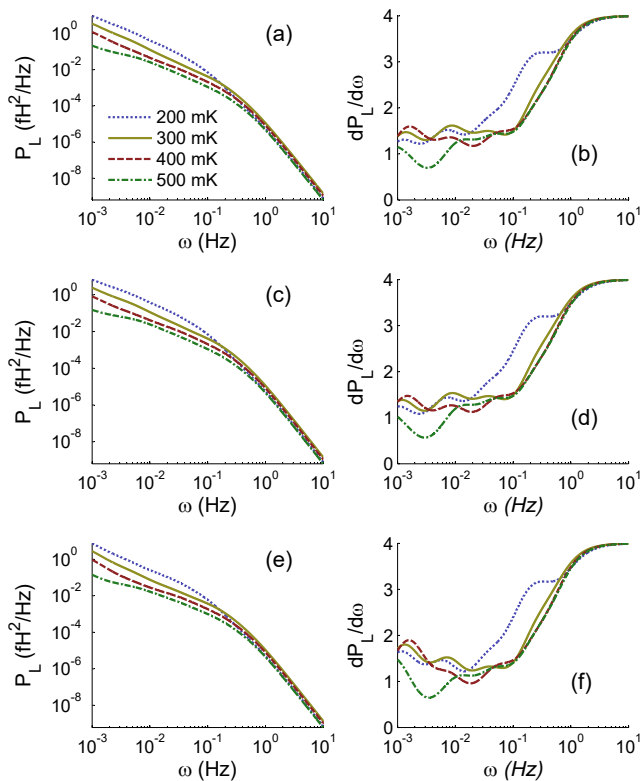


Figure 9. Inductance noise plots for different $\Delta\nu = \omega_b - \omega_a$ showing the (a) Power-spectrum and (b) its respective slope for $\omega_b = 10$ Hz and $\omega_a = 10^{-3}$ Hz. (c) Power-spectrum and (d) its respective slope for $\omega_b = 10$ Hz and $\omega_a = 10^{-2}$ Hz. (e) Power-spectrum and (f) its respective slope for $\omega_b = 10$ Hz and $\omega_a = 10^{-1}$ Hz. Calculations are for 400 cluster with 6-9 spins.

Eq.27 is used for the numerical inductance noise calculations for the ensemble of spin-clusters. The T-dependent inductance noise spectrum and its slope is shown in fig.9 for different $\Delta\nu = \omega_b - \omega_a$, since second spectrum calculations are sensitive to $\Delta\nu$. In subplots fig.9-(a) and (b) nearly the whole spectrum is covered. While in the other subplots the ω_a is consecutively reduced by an order of magnitude. Varying ω_a affects the power spectrum more than varying ω_b . It is shown that when $\Delta\nu$ nearly covers the full spectrum, the noise power spectrum now shows $1/f^\alpha$ behavior at intermediate frequencies. The average integrated α between $0.001 - 0.05$ Hz varies from ~ 1.57 (at 200 mK) to ~ 1.24 (at 500 mK). As the temperature further increases $\alpha \rightarrow 0$. The $\alpha = 4$ at high frequencies is due to the square of the Lorentzian tail while at the lowest frequencies α eventually rolls over to zero. Overall the inductance noise shows a large variation with temperature and the calculations agree very well with experiment^{39,42}.

IV. SUMMARY

Overall a self-consistent model proposed here explains various observed features of the temperature dependent $1/f^{\alpha(T)}$

magnetization noise in SQUIDs. With no a priori assumptions on a log normal distribution of fluctuation rates, it is shown that $1/f^\alpha$ noise can be obtained, at low temperatures, for a ferromagnetically interacting defect model. In this model multiple finite sized spin clusters representing spatial disorder where each cluster is magnetically ordered by ferromagnetic RKKY interactions. Both, a random normal distribution of cluster sizes and ferromagnetic long range interactions are essential for obtaining the $1/f^\alpha$ type power spectrum. The flux noise is shown to be independent of system size.

It is shown that the $1/f$ noise occurs at the onset of a second order thermodynamic phase transition for finite sized spin clusters. The noise exponent α (considered over some spectral range) is constant over a short range of temperatures when the clusters are still magnetically ordered. α then rapidly drops as the system heads towards criticality. This behavior is reminiscent of Bak's famous argument that $1/f$ noise manifests in spatially extended metastable dynamical systems²¹

The magnetic ordering is further verified self-consistently through three-point correlations, namely the flux-inductance noise cross power spectrum. This non-zero cross power spectrum confirms the breaking of time reversal symmetry by the clusters at temperatures where $\alpha \sim 1$.

Finally, based on the fluctuation dissipation theorem, it is analytically shown why the inductance noise is inherently T^{-2} dependent while the flux noise is not. Calculated cross-correlations between flux- and inductance-noise with ferromagnetic RKKY interactions shows that there is a magnetically ordered phase for the TLS, as seen in experiment³⁹. A method suggested here for obtaining n -point correlation functions is key to these calculations. Analytical expressions are provided for easier four-point correlation function calculations.

In this paper a recent method is used for calculating the temperature dependent noise spectra of interacting TLSs. The TLSs are modeled as flip-flopping Ising spins whose temperature dependent fluctuations are governed by Glauber dynamics. A method is suggested here to systematically extract any n^{th} -order correlation function, from the solutions of the stochastic master equation, for N arbitrary TLSs. This model is fully consistent with the usual method of calculating $1/f$ noise from random telegraphic signals. Further, this model complements the existing method by adding interactions and temperature dependence and providing the option of not assuming any distribution for the flip rate. Besides numerics, a number of analytical expressions are derived based on this method.

V. APPENDIX-A

A. Analytic Expressions for Two Correlated TLS

Analytical expressions are provided for the auto-correlation functions, cross-correlation functions and the power spectrum for a pair of interacting spins using this paper's model.

Master Equations: If the average occupation of the two states is the same (for unbiased fluctuators), then for single

spin- i $\mathbf{V}_i = \gamma_i(\sigma_x - \sigma_o)$, where γ_i is the i^{th} spin's relaxation rate. The corresponding flipping probability matrix is

$$\mathbf{W}_i(t) = \exp(\mathbf{V}_i t) = \frac{1 + e^{-2\gamma_i t}}{2} \sigma_o + \frac{1 - e^{-2\gamma_i t}}{2} \sigma_x. \quad (28)$$

For N uncorrelated (non-interacting) Ising spins, it is straightforward to express the entire system's flipping probability matrix as a tensor product of individual \mathbf{W}_i s:

$$\mathbf{W} = \mathbf{W}_1 \otimes \mathbf{W}_2 \otimes \dots \otimes \mathbf{W}_N \quad (29)$$

The matrix $\mathbf{V} = \dot{\mathbf{W}}\mathbf{W}^{-1}$ which is also

$$\mathbf{V} = - \sum_j \gamma_j \mathbf{I} + \sum_j \gamma_j \sigma_x^{(j)} \quad (30)$$

where \mathbf{I} is the identity matrix. For self consistency it can be verified that this is the same as what is obtained from Eq.2 in the $T \rightarrow \infty$ limit.

Correlated TLS Fluctuations: In order to obtain the power spectrum of a given pair of interacting TLSs or Ising spins, the corresponding two point correlation functions have to be obtained first. Consider the Ising-Glauber model outlined in the main body of the paper for two fluctuating Ising spins that are correlated. If $B = 0$, then the \mathbf{V} matrix in the $\{11, 1\bar{1}, \bar{1}1, \bar{1}\bar{1}\}$ basis has the following form

$$\mathbf{V} = \frac{2}{\varepsilon} \begin{bmatrix} -\sum_i \gamma_i & \gamma_2 \varepsilon' & \gamma_1 \varepsilon' & 0 \\ \gamma_2 & -\varepsilon' \sum_i \gamma_i & 0 & \gamma_1 \\ \gamma_1 & 0 & -\varepsilon' \sum_i \gamma_i & \gamma_2 \\ 0 & \gamma_1 \varepsilon' & \gamma_2 \varepsilon' & -\sum_i \gamma_i \end{bmatrix} \quad (31)$$

or

$$\mathbf{V} = \mathbf{V}_o \times \left[I + \tanh(\beta J) \sigma_z^{(1)} \sigma_z^{(2)} \right] \quad (32)$$

where $\varepsilon' = \exp(2\beta J)$ and $\varepsilon = 1 + \exp(2\beta J)$ and

$$\mathbf{V}_o = \gamma_1 \sigma_x^{(1)} + \gamma_2 \sigma_x^{(2)} - (\gamma_1 + \gamma_2) \mathbf{I} \quad (33)$$

Obviously if $\beta J = 0$, then $\mathbf{V} = \mathbf{V}_o$ which is just the \mathbf{V} matrix for two uncorrelated TLS. Also $\sigma_x^{(1)} = \sigma_x \otimes \sigma_o$ and $\sigma_x^{(2)} = \sigma_o \otimes \sigma_x$.

The autocorrelation functions and the cross-correlation functions now are:

$$\begin{aligned} \langle s_1(0) s_1(t) \rangle &= \langle \mathbf{f} | \sigma_z^{(1)} \mathbf{W}(t) \sigma_z^{(1)} \mathbf{W}(0) | \mathbf{i} \rangle \\ &= [\cosh(\Theta t) + K_{11} \sinh(\Theta t)] e^{-\sum \gamma_i t} \end{aligned} \quad (34)$$

$$\begin{aligned} \langle s_2(0) s_1(t) \rangle &= \langle \mathbf{f} | \sigma_z^{(2)} \mathbf{W}(t) \sigma_z^{(1)} \mathbf{W}(0) | \mathbf{i} \rangle \\ &= \tanh(2J\beta) [\cosh(\Theta t) + K_{21} \sinh(\Theta t)] e^{-\sum \gamma_i t} \end{aligned} \quad (35)$$

where $\mathbf{W} = \exp(-\mathbf{V}t)$, $\Theta = \zeta/\varepsilon$ and $\zeta = \sqrt{(\gamma_1 + \gamma_2)^2 \varepsilon^2 - 16\gamma_1 \gamma_2 (\varepsilon - 1)}$ and

$$K_{11} = \varepsilon \frac{\gamma_1(\varepsilon^2 - 6\varepsilon + 6) + \gamma_2(\varepsilon^2 - 2\varepsilon + 2)}{\zeta(2 - 2\varepsilon + \varepsilon^2)} \quad (36)$$

$$K_{21} = \frac{4(1 - \varepsilon)\gamma_2 + \varepsilon^2(\gamma_1 + \gamma_2)}{\zeta \varepsilon} \quad (37)$$

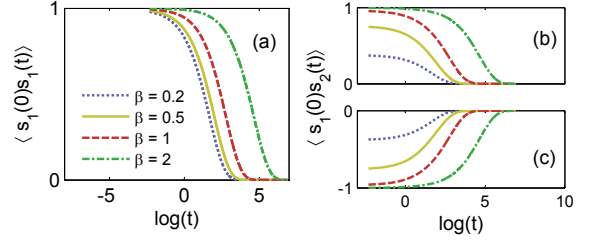


Figure 10. Temperature dependent (a) autocorrelation functions, (b) cross-correlation functions for $J = 1$, (c) cross-correlation functions for $J = -1$ for an interacting pair of fluctuators, shown for $\gamma_1 = 0.1$ and $\gamma_2 = 0.2$.

Here the projection vectors corresponding to the zero eigenvalue solution of \mathbf{V} are:

$$|i\rangle = |f\rangle = \frac{1}{\sqrt{2 + 2(1 - \varepsilon)^2}} [\varepsilon - 1, 1, 1, \varepsilon - 1] \quad (38)$$

The sum of all cross- and auto-correlation functions have the form:

$$\sum_{j,k} \langle s_j(0) s_k(t) \rangle = K_+ e^{-\Gamma_+ |t|} + K_- e^{-\Gamma_- |t|} \quad (39)$$

where

$$K_{\pm} = (2 \pm K_{11} \pm K_{22}) + \tanh(2\beta J) (2 \pm K_{12} \pm K_{21}) \quad (40)$$

and

$$\Gamma_{\pm} = \gamma_1 + \gamma_2 \pm \zeta/\varepsilon \quad (41)$$

Power Spectrum: The temperature dependent autocorrelation functions are shown in Fig.10-(a) and the cross-correlation functions are shown for ferromagnetic interactions in Fig.10-(b) and anti-ferromagnetic interactions in Fig.10-(c). As expected for anti-ferromagnetic interactions, the cross-correlation function is anti-correlated for a pair of fluctuators at initial times, whereas the autocorrelation function does not depend on the sign of J . Also note that the maximum amplitude of the cross-correlation function is inversely proportional to the temperature as expected. Thereby ensuring that the cross-correlation terms vanish at high temperatures.

The respective power spectra are obtained by taking the Fourier transform of the correlation functions Eqs.35-36,

$$P_{ij}(\omega) = \int_0^{\infty} \langle s_i(0) s_j(t) \rangle e^{i\omega t} dt \quad (42)$$

and therefore

$$P_{11}(\omega) = \tilde{P}_+ + K_{11} \tilde{P}_- \quad (43)$$

$$P_{21}(\omega) = \tanh(2J\beta) \left[\tilde{P}_+ + K_{21} \tilde{P}_- \right] \quad (44)$$

where

$$\tilde{P}_{\pm} = \frac{\Gamma_-}{\Gamma_-^2/2 + \omega^2} \pm \frac{\Gamma_+}{\Gamma_+^2/2 + \omega^2} \quad (45)$$

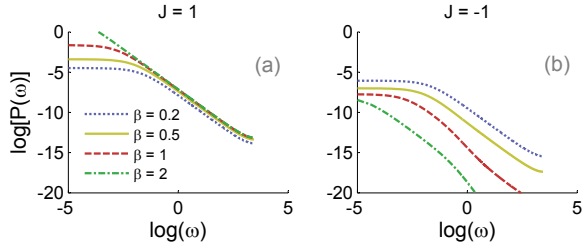


Figure 11. Temperature dependent power spectrum for a pair of fluctuators, with $\gamma_1 = 0.1$ and $\gamma_2 = 0.2$, shown for (a) $J = 1$ ferromagnetic interaction and (b) $J = -1$ anti-ferromagnetic interaction.

Similarly, expressions for P_{22} and P_{21} can be obtained by swapping the indices 1 and 2 in the above expressions for the power spectrum and also for the respective coefficients. The total power spectrum, for the pair of spins, is then just the total

$$\mathbf{W} = \frac{1}{2\varepsilon} \begin{bmatrix} \varepsilon' e^{-4t} + \varepsilon e^{-4t\varepsilon'/\varepsilon} + 1, & 1 - e^{-4t}, & 1 - e^{-4t}, & \varepsilon' e^{-4t} - \varepsilon e^{-4t\varepsilon'/\varepsilon} + 1 \\ -\varepsilon'(e^{-4t} - 1), & e^{-4t} + \varepsilon(1 + e^{-4t/\varepsilon}) - 1, & e^{-4t} + \varepsilon(1 - e^{-4t/\varepsilon}) - 1, & -\varepsilon'(e^{-4t} - 1) \\ -\varepsilon'(e^{-4t} - 1), & e^{-4t} + \varepsilon(1 - e^{-4t/\varepsilon}) - 1, & e^{-4t} + \varepsilon(1 + e^{-4t/\varepsilon}) - 1, & -\varepsilon'(e^{-4t} - 1) \\ \varepsilon' e^{-4t} - \varepsilon e^{-4t\varepsilon'/\varepsilon} + 1, & 1 - e^{-4t}, & 1 - e^{-4t}, & \varepsilon' e^{-4t} + \varepsilon e^{-4t\varepsilon'/\varepsilon} + 1 \end{bmatrix} \quad (47)$$

This gives the corresponding correlation functions for two interacting TLS:

$$\langle s_i(0)s_j(t) \rangle = \frac{1}{2} e^{-2\Gamma'_- |t|} + \left(\delta_{ij} - \frac{1}{2} \right) e^{4\beta J} e^{-2\Gamma'_+ |t|} \quad (48)$$

where $\Gamma'_\pm = [1 + \exp(\pm 2\beta J)]^{-1}$. Note that here, $\sum_{ij} \langle s_i(0)s_j(t) \rangle = 2e^{-2\Gamma'_- |t|}$. This implies that in this special case the two interacting TLS can be expressed as a single effective TLS with flipping rate Γ'_- .

B. Typical Method to Obtain $1/f$ noise

Usually for $1/f$ noise a log normal distribution of the fluctuations rates is assumed. In the presence of several uncorrelated TLSs, the power spectrum from the two point correlation

sum $P(\omega) = \sum_{i,j} P_{ij}(\omega)$, where $i, j = 1, 2$ and is shown in Fig.11 for various ferromagnetic and anti-ferromagnetic interactions. It is seen that for the ferromagnetic case, $J = 1$, the amplitude of the power spectra is inversely proportional to the temperature whereas for $J = -1$ it is directly proportional. In general one can solve for the systems dynamics by evaluating the eigenvalues and eigenvectors of the \mathbf{V} matrix directly for a large number of spins. However this quickly becomes a prohibitive as the size of \mathbf{V} scales as 2^N (N being the total number of TLSs).

Limits: In the infinite temperature limit $\lim_{T \rightarrow \infty} \zeta/\varepsilon = \gamma_1 + \gamma_2$. Cross-correlations (Eq.36) are zero and the two-point autocorrelation function Eq.35 just reduces to that of two uncorrelated Ising spins/TLS:

$$\langle s_i(0)s_j(t) \rangle = \delta_{ij} e^{-2\gamma_i t} \quad (46)$$

Whereas at finite temperatures and in the $\gamma_j = 1$ limit, the flipping probability matrix has the following form:

functions is

$$P(\omega) = \int_0^\infty \int_0^\infty D(\gamma) e^{-2\gamma t} e^{-i\omega t} dt d\gamma \quad (49)$$

$$= \int_0^\infty D(\gamma) \frac{2\gamma}{\omega^2 + 4\gamma^2} d\gamma \quad (50)$$

If the distribution $D(\gamma) \propto \gamma^{-1}$ in some range $\gamma_{min} < \gamma < \gamma_{max}$, then

$$P(\omega) = \frac{1}{\omega} \left[\arctan\left(\frac{2\gamma_{max}}{\omega}\right) - \arctan\left(\frac{2\gamma_{min}}{\omega}\right) \right] \quad (51)$$

Here $P(\omega) \propto \omega^{-1}$ when $2\gamma_{min} < \omega < 2\gamma_{max}$ since the term in the square parenthesis is ~ 1 in that range.

VI. ACKNOWLEDGEMENTS

My deepest thanks to Robert Joynt for several invaluable discussions. Very special thanks to Robert McDermott for carefully discussing the experiments. Also my sincere thanks to Leonid Pryadko.

¹ W. Schottky, Phys. Rev. **28**, 74 (1926).

² P. Dutta and P. M. Horn, Rev. Mod. Phys. **53**, 497 (1981).

³ M. B. Weissman, Rev. Mod. Phys. **60**, 537 (1988).

- ⁴ E. Paladino, M. Galperin, Y. G. Falci, and L. Altshuler, B., Rev. Mod. Phys. **86**, 361 (2014).
- ⁵ J. G. Massey and M. Lee, Phys. Rev. Lett. **79**, 3986 (1997).
- ⁶ J. Wu, T. Tshepe, J. E. Butler, and M. J. R. Hoch, Phys. Rev. B **71**, 113108 (2005).
- ⁷ M. B. Weissman, Rev. Mod. Phys. **65**, 829 (1993).
- ⁸ K. Shtengel and C. C. Yu, Phys. Rev. B **67**, 165106 (2003).
- ⁹ A. Shumilin, Solid State Communications **183**, 51 (2014), ISSN 0038-1098.
- ¹⁰ R. F. Voss and J. Clarke, Phys. Rev. B **13**, 556 (1976).
- ¹¹ J. V. Mantese and W. W. Webb, Phys. Rev. Lett. **55**, 2212 (1985).
- ¹² G. A. Garfunkel, G. B. Alers, M. B. Weissman, J. M. Mochel, and D. J. VanHarlingen, Phys. Rev. Lett. **60**, 2773 (1988).
- ¹³ C. T. Rogers and R. A. Buhrman, Phys. Rev. Lett. **53**, 1272 (1984).
- ¹⁴ P. Handel, Electron Devices, IEEE Transactions on **41**, 2023 (1994), ISSN 0018-9383.
- ¹⁵ M. J. Uren, D. J. Day, and M. J. Kirton, Applied Physics Letters **47** (1985).
- ¹⁶ Y. Lai, H. Li, D. K. Kim, B. T. Diroll, C. B. Murray, and C. R. Kagan, ACS Nano **8**, 9664 (2014), pMID: 25195975.
- ¹⁷ K.-M. Persson, B. G. Malm, and L.-E. Wernersson, Applied Physics Letters **103**, 033508 (2013).
- ¹⁸ A. Balandin, S. Morozov, S. Cai, R. Li, K. Wang, G. Wijeratne, and C. Viswanathan, Microwave Theory and Techniques, IEEE Transactions on **47**, 1413 (1999), ISSN 0018-9480.
- ¹⁹ A. A. Kaverzin, A. S. Mayorov, A. Shtyov, and D. W. Horsell, Phys. Rev. B **85**, 075435 (2012).
- ²⁰ A. A. Balandin, Nature nanotechnology **8**, 549 (2013).
- ²¹ P. Bak, C. Tang, and K. Wiesenfeld, Phys. Rev. Lett. **59**, 381 (1987).
- ²² S. Kogan, *Electronic Noise and Fluctuations in Solids* (Cambridge University Press, 1996).
- ²³ Y. M. Galperin, B. L. Altshuler, J. Bergli, and D. V. Shantsev, Phys. Rev. Lett. **96**, 097009 (2006).
- ²⁴ B. Bellomo, R. Lo Franco, and G. Compagno, Phys. Rev. A **77**, 032342 (2008).
- ²⁵ J. Dajka, M. Mierzejewski, and J. Łuczka, Phys. Rev. A **77**, 042316 (2008).
- ²⁶ G. Burkard, Phys. Rev. B **79**, 125317 (pages 6) (2009).
- ²⁷ D. Zhou and R. Joynt, Phys. Rev. A **81**, 010103 (2010).
- ²⁸ L. M. K. Vandersypen, J. M. Elzerman, R. N. Schouten, L. H. W. van Beveren, R. Hanson, and L. P. Kouwenhoven, Appl. Phys. Lett. **85**, 4394 (2004).
- ²⁹ K. MacLean, S. Amasha, I. P. Radu, D. M. Zumbühl, M. A. Kastner, M. P. Hanson, and A. C. Gossard, Phys. Rev. Lett. **98**, 036802 (2007).
- ³⁰ D. Taubert, M. Pioro-Ladrière, D. Schröer, D. Harbusch, A. S. Sachrajda, and S. Ludwig, Phys. Rev. Lett. **100**, 176805 (2008).
- ³¹ G. Wendin and V. S. Shumeiko, Low Temperature Physics **33**, 724 (2007).
- ³² F. Yoshihara, K. Harrabi, A. O. Niskanen, Y. Nakamura, and J. S. Tsai, Phys. Rev. Lett. **97**, 167001 (2006).
- ³³ R. C. Bialczak, R. McDermott, M. Ansmann, M. Hofheinz, N. Katz, E. Lucero, M. Neeley, A. D. O'Connell, H. Wang, A. N. Cleland, et al., Phys. Rev. Lett. **99**, 187006 (2007).
- ³⁴ R. H. Koch, J. Clarke, W. M. Goubau, J. M. Martinis, C. M. Pegrum, and D. J. Harlingen, Journal of Low Temperature Physics **51**, 207 (1983), ISSN 0022-2291, 10.1007/BF00683423.
- ³⁵ F. Wellstood, C. Urbina, and J. Clarke, Magnetism, IEEE Transactions on **23**, 1662 (1987), ISSN 0018-9464.
- ³⁶ S. Oh, K. Cicak, J. S. Kline, M. A. Sillanpää, K. D. Osborn, J. D. Whittaker, R. W. Simmonds, and D. P. Pappas, Phys. Rev. B **74**, 100502 (2006).
- ³⁷ P. Kumar, S. Sendelbach, M. A. Beck, J. W. Freeland, Z. Wang, H. Wang, C. C. Yu, R. Q. Wu, D. P. Pappas, and R. McDermott, Phys. Rev. Applied **6**, 041001 (2016).
- ³⁸ T. Lanting, A. J. Berkley, B. Bumble, P. Bunyk, A. Fung, J. Johansson, A. Kaul, A. Kleinsasser, E. Ladizinsky, F. Maibaum, et al., Phys. Rev. B **79**, 060509 (2009).
- ³⁹ S. Sendelbach, D. Hover, A. Kittel, M. Mück, J. M. Martinis, and R. McDermott, Phys. Rev. Lett. **100**, 227006 (2008).
- ⁴⁰ H. Bluhm, J. A. Bert, N. C. Koshnick, M. E. Huber, and K. A. Moler, Phys. Rev. Lett. **103**, 026805 (2009).
- ⁴¹ R. McDermott, Applied Superconductivity, IEEE Transactions on **19**, 2 (2009), ISSN 1051-8223.
- ⁴² F. Wellstood, C. Urbina, and J. Clarke, Applied Superconductivity, IEEE Transactions on **21**, 856 (2011), ISSN 1051-8223.
- ⁴³ S. Choi, D.-H. Lee, S. G. Louie, and J. Clarke, Phys. Rev. Lett. **103**, 197001 (2009).
- ⁴⁴ R. H. Koch, D. P. DiVincenzo, and J. Clarke, Phys. Rev. Lett. **98**, 267003 (2007).
- ⁴⁵ R. de Sousa, Phys. Rev. B **76**, 245306 (2007).
- ⁴⁶ L. F. K. Kechedzhi and L. B. Ioffe, ArXiv p. 1102.3445 (2011).
- ⁴⁷ S. LaForest and R. de Sousa, Phys. Rev. B **92**, 054502 (2015).
- ⁴⁸ V. I. Kozub, Solid State Communications **97**, 843 (1996), ISSN 0038-1098.
- ⁴⁹ L. Faoro and L. B. Ioffe, Phys. Rev. Lett. **100**, 227005 (2008).
- ⁵⁰ Solid State Communications **33**, 273 (1980), ISSN 0038-1098.
- ⁵¹ B. I. Shklovskii, Phys. Rev. B **67**, 045201 (2003).
- ⁵² A. De, Advances in Condensed Matter Physics **2015** (2015).
- ⁵³ Z. Chen and C. C. Yu, Phys. Rev. Lett. **104**, 247204 (2010).
- ⁵⁴ A. Sundaresan, R. Bhargavi, N. Rangarajan, U. Siddesh, and C. N. R. Rao, Phys. Rev. B **74**, 161306 (2006).
- ⁵⁵ G. Yang, D. Gao, J. Zhang, J. Zhang, Z. Shi, and D. Xue, The Journal of Physical Chemistry C **115**, 16814 (2011).
- ⁵⁶ P. R. L. Keating, D. O. Scanlon, and G. W. Watson, Journal of Physics: Condensed Matter **21**, 405502 (2009).
- ⁵⁷ M. Venkatesan, C. B. Fitzgerald, and J. M. D. Coey, Nature **430**, 630 (2004).
- ⁵⁸ X. Han, J. Lee, and H.-I. Yoo, Phys. Rev. B **79**, 100403 (2009).
- ⁵⁹ G. S. Chang, J. Forrest, E. Z. Kurmaev, A. N. Morozovska, M. D. Glinchuk, J. A. McLeod, A. Moewes, T. P. Surkova, and N. H. Hong, Phys. Rev. B **85**, 165319 (2012).
- ⁶⁰ H. Wang, C. Shi, J. Hu, S. Han, C. C. Yu, and R. Q. Wu, Phys. Rev. Lett. **115**, 077002 (2015).
- ⁶¹ D. Lee, J. L. DuBois, and V. Lordi, Phys. Rev. Lett. **112**, 017001 (2014).
- ⁶² Z. Wang, H. Wang, C. C. Yu, and R. Wu, arXiv preprint arXiv:1709.06208 (2017).
- ⁶³ A. De, Phys. Rev. Lett. **113**, 217002 (2014).
- ⁶⁴ B. Cheng, Q.-H. Wang, and R. Joynt, Phys. Rev. A **78**, 022313 (2008).
- ⁶⁵ R. Joynt, D. Zhou, and Q.-H. Wang, International Journal of Modern Physics B **25**, 2115 (2011).
- ⁶⁶ D. Zhou, A. Lang, and R. Joynt, Quantum Inf Process (2010).
- ⁶⁷ A. De, A. Lang, D. Zhou, and R. Joynt, Phys. Rev. A **83**, 042331 (2011).
- ⁶⁸ D. Zhou and R. Joynt, Superconductor Science and Technology **25**, 045003 (2012).
- ⁶⁹ A. De and R. Joynt, Phys. Rev. A **87**, 042336 (2013).
- ⁷⁰ N. G. V. Kampen, *Stochastic Processes in Physics and Chemistry* (Elsevier, Amsterdam, 2007), 3rd ed.
- ⁷¹ R. J. Glauber, Journal of Mathematical Physics **4** (1963).
- ⁷² Y. Ozeki, Journal of Physics: Condensed Matter **9**, 11171 (1997).
- ⁷³ W. Reim, R. H. Koch, A. P. Malozemoff, M. B. Ketchen, and H. Maletta, Phys. Rev. Lett. **57**, 905 (1986).

⁷⁴ S. Vitale, G. A. Prodi, and M. Cerdonio, *J. Appl. Phys.* **65**, 2130 (1989).

⁷⁵ D. McCammon, M. Galeazzi, D. Liu, W. Sanders, B. Smith, P. Tan, K. Boyce, R. Brekosky, J. Gygax, R. Kelley, et al., *physica status solidi (b)* **230**, 197 (2002), ISSN 1521-3951.

⁷⁶ A. K. Nguyen and S. M. Girvin, *Phys. Rev. Lett.* **87**, 127205 (2001).